NASA DEVELOP National Program
Massachusetts – Boston
Spring 2022

Padre Island Water Resources

Monitoring Historic Shoreline Change and Suspended Sediment Patterns along Padre Island National Seashore

DEVELOP Technical Report
Final – March 31st, 2022

Lisa Tanh (Project Lead)
Yuhe Chang
Rachel Lazzaro
Cameron Reimer

Advisor:
Dr. Cedric Fichot, Boston University (Science Advisor)

1. Abstract

Land loss along Padre Island National Seashore threatens the safety of the recreational beach for the general public and endangers wildlife habitats and nesting sites. Historically, the Army Corps of Engineers has conducted dredging efforts to thwart erosion. Quantifying spatial and temporal variations of shoreline change is vital to understanding the interaction of land loss and historical dredging efforts. NASA DEVELOP collaborated with the National Park Service to use remote sensing to investigate the impact of dredging on Padre Island National Seashore's shoreline. The team utilized high-resolution imagery from Maxar and Planet to create a time series of shoreline changes between 2011 and 2020, conduct shoreline extraction, and quantify shoreline changes. Additionally, the team monitored turbidity and sediment dynamics using Landsat 8 Operational Land Imager (OLI), Landsat 4 Thematic Mapper (TM), Landsat 5 TM, and Sentinel-2 MultiSpectral Instrument (MSI). Shoreline change results demonstrated an average change between 4.5 to 32 meters annually. Meanwhile, the dredging area directly north of the seashore's Port Mansfield Channel experienced an areal gain of 152,000 m^2 between 2010 and 2021. The team also observed that turbidity values increased in areas close to the channel where dredging occurred, especially in the 2018 and 2021 dredging years. Dredging years corresponded with less shoreline change than years without dredging. These results will be used to better inform future partner-designed shoreline management projects in the face of continued erosion and sea level rise.

Key Terms

remote sensing, coastal erosion, turbidity, barrier island, Landsat, Maxar, Planet

2. Introduction

2.1 Background Information

Padre Island National Seashore is an undeveloped, 66-mile-long barrier island located off the coast of South Texas (Figure 1), which encompasses dunes, prairies, and tidal flats (Bracewell, 2017). The island is home to local wildlife, including nesting sea turtles, and is a recreational beach for the general public. Since 1962, Padre Island National Seashore has experienced shoreline erosion as a result of the construction of jetties at the Port Mansfield Channel (Morton, 1975). The erosion narrows the width of the beach and causes pinch points and flooding— a safety threat to visitors of the beach. The island's biodiversity is threatened by erosion which contributes to the loss of habitat and nesting domain of endangered sea turtles, one of the many threatened species on the island. Storms, such as Hurricane Hanna of 2020, have further increased the erosion of the beach and implicated a need for beach management efforts. Dredging projects have been continuously implemented by the United States Army Corps of Engineers to slow erosion, however, more information is needed to determine the effectiveness of consistent dredging projects. Understanding the effects of these dredging projects, as well as natural weather occurrences, on shoreline erosion is a crucial component of informed decision-making for shoreline management of the park.

To address these concerns, the NASA DEVELOP Massachusetts team used remote sensing and geospatial analysis to monitor the changes in coastline and turbidity over time. Many studies have had success in coastline delineation through a

variety of methods; these methods include both supervised and unsupervised classification methods, as well as those that utilize the spectral properties of both land and water for delineation (Toure et al, 2019; Ghorai & Mahapatra, 2020; Domazetović et al, 2021). While manual delineation of shoreline imagery may increase accuracy, it is exceptionally time-consuming. The team explored different methods of automating shoreline extraction based on commonly used methodologies from literature recommendations. In particular, the team focused on two separate forms of classification and a thresholding method using a ratio derived from spectral bands for analysis of both Maxar and Planet data. These measured changes in the coastline were compared with the timeline of dredging projects to understand the implications of dredging on the region's shoreline. The average distance of shoreline change was computed within a 10-mile span, as well as the average area change within a 1.4-mile region north of the Port Mansfield Channel. With regards to sediments, turbidity at the ocean-facing nearshore region of Padre Island is largely unknown as a result of limited *in situ* turbidity data collection. While *in situ* measurements are the usual methodology in understanding sediment dynamics, remote sensing estimations are useful in situations where obtaining timely samples is not possible due to geographic or economic constraints. To address this data gap at Padre Island, the team utilized an aquatic-based atmospheric correction and a remote sensing algorithm designed to measure turbidity and sediment suspension (Dogliotti, 2015). The algorithm selected is particularly suited to the retrieval of turbidity values in coastal and estuarine waters, making its use in the Padre Island nearshore environment a better fit than other remote sensing techniques of turbidity and suspended sediment estimation.

2.1.1 Study Area & Period

The team's study area focused on the Port Mansfield Channel and the adjacent 10 miles north of the channel. This part of the island showed a significant loss of land and has been highly affected by previous dredging projects, largely as a result of the jetties (Bracewell, 2019). The study period for the shoreline analysis encompassed the years 2011–2021. This period was chosen to observe the effects of known dredging projects on the Port Mansfield Channel using data of the highest spatial resolution. For the turbidity analysis the team focused on the years 2005 and 2010–2022.

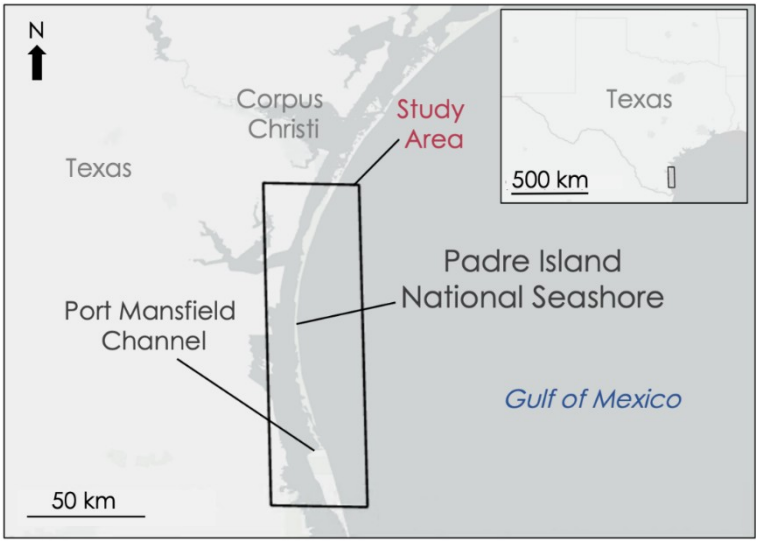


Figure 1: Study area map of Padre Island National Seashore, Texas.

2.2 Project Partners & Objectives

The team partnered with the National Park Service (NPS) on this project. The National Park Service manages the beach of Padre Island by monitoring and overseeing occasional dredging events provided by the Army Corp of Engineers. Padre Island National Seashore, managed by the NPS, is interested in this project because they sought information on the effect of dredging events on shoreline change rates in order to choose the most effective dredging method. This project aimed to provide partners at Padre Island National Seashore with an informative overview of sediment deposition trends and shoreline change in recent years using satellite data. The first objective was to create a time series of high-resolution maps to visualize the shoreline throughout time. The team compared the shoreline change time series and dredge history to understand the effects of dredging on shoreline loss or accretion along Padre Island National Seashore. Evaluating this relationship also provides insight to plan dredging frequency and priority locations. The second objective was to create a time series of turbidity to understand suspended sediment patterns throughout time. The turbidity time series provided partners with seasonal variability information on sediment transport and sediment direction post dredging.

3. Methodology

3.1 Data Acquisition

3.1.1 High-Resolution Image Acquisition

The team acquired high-resolution imagery for the shoreline change analysis from Maxar (Neigh et al., 2013) and Planet. All Maxar images obtained were at 0.7-meter spatial resolution and from the WorldView and Geoeye missions. All Planet images were at 3-meter spatial resolution and from the PlanetScope mission. The team obtained one image from the Maxar archive for nearly each year from 2010 through 2021; several images from Planet were obtained from 2019 through 2021. The acquisition dates and platforms of the high-resolution imagery are listed in Table 1.

Table 1:
Acquisition information of high-resolution data utilized for the shoreline analysis.

Platform	Mission	Acquisition Date
Maxar	WorldView-2	9/16/2010, 7/23/2011, 6/16/2012, 8/2/2013, 7/16/2014, 9/1/2016, 7/31/2020
Maxar	WorldView-3	7/11/2015, 6/3/2017, 10/29/2021
Maxar	Geoeye	8/1/2018
Planet	PlanetScope	10/26/2019, 12/22/2019, 6/11/2020, 2/3/2021, 4/20/2021

3.1.2 Landsat and Sentinel Image Acquisition
All data the team collected for turbidity analysis were multispectral imagery products from Landsat and Sentinel missions (Table 2) and downloaded from USGS/EROS Inventory Service using its Python API. In order to cover the study area, the team collected two tiles at Landsat path 26, rows 40 and 41. For the subsequent turbidity analysis that focused on the years 2005 and 2010 – 2022, they collected approximately 20 images per year. All imagery selected for download were subject to a 50% cloud cover limit.

Table 2:
Earth observation platforms, sensors, level, and dates of image captured.

Platform	Sensor	Level	Dates of Image Capture	Parameters Examined
Landsat 5	Thematic Mapper (TM)	Level-1	2005, 2010 – 2013	Water turbidity
Landsat 8	Operational Land Imager (OLI)	Level-1	2014 – 2020	Water turbidity
Sentinel-2	MultiSpectral Instrument (MSI)	Level-2A	2015 – 2020	Water turbidity

3.1.3 In situ Data Acquisition
The team received in situ turbidity measurements spanning across more than 15 years (Jan. 2004 ~ Feb. 2022) from Dr. Philippe Tissot at Texas A&M University–Corpus Christi which compared with the retrieved turbidity values from multispectral imagery. There are three buoy stations where the *in situ* measurements are collected. The team used one station, the Bird Island Basin

station (#171, 27° 29' 4" N, 97° 19' 5" W), because the other buoy locations were outside the extent of the team's study area.

3.2 Data Processing for Shoreline and Turbidity Analysis

For the shoreline analysis, the team processed the high-resolution imagery by mosaicing, georectifying, and adjusting for color and sharpness. First, the team mosaiced the Maxar and Planet high-resolution imagery using the Raster Merge tool in QGIS. After processing, some images had a significant offset at tile merging locations. Due to the project's limited time span, a definitive resolution of the offset error was not possible. The locations of the offsets were noted and areas north of the error were excluded from the shoreline analysis. Next, the team georectified the mosaiced imagery prior to analysis to ensure accurate geographic locations. To create GPS points for georectification, the team manually selected easily recognizable points from an aerial imagery dataset "Texas NAIP Imagery" downloaded from the National Agriculture Imagery Program (NAIP). Then they shifted the high-resolution imagery to match these points using the Geospatial Data Abstraction Library's (GDAL) Translate script, available in the Open-Source Geospatial Foundation (OSGeo) shell. Lastly, the team adjusted the color and sharpness to improve image clarity prior to applying the classification and Normalized Difference Water Index (NDWI) methodologies. For the turbidity analysis, the team processed Landsat 4-5 TM, Landsat 8 OLI, and Sentinel-2 turbidity imagery in Atmospheric Correction for Operational Land Imager lite (ACOLITE) using a single algorithm developed by Dogliotti et al. (2015) (Appendix A). Processed turbidity imagery from ACOLITE was visualized as static maps in SeaWiFS Data Analysis Systems (SeaDAS).

3.3 Data Analysis

3.3.1 Data Analysis for Shoreline Change

To analyze shoreline change, the team used three separate methodologies to digitize the coastline near the Port Mansfield Channel: random forest classification, iso cluster classification, and band ratio of the NDWI.

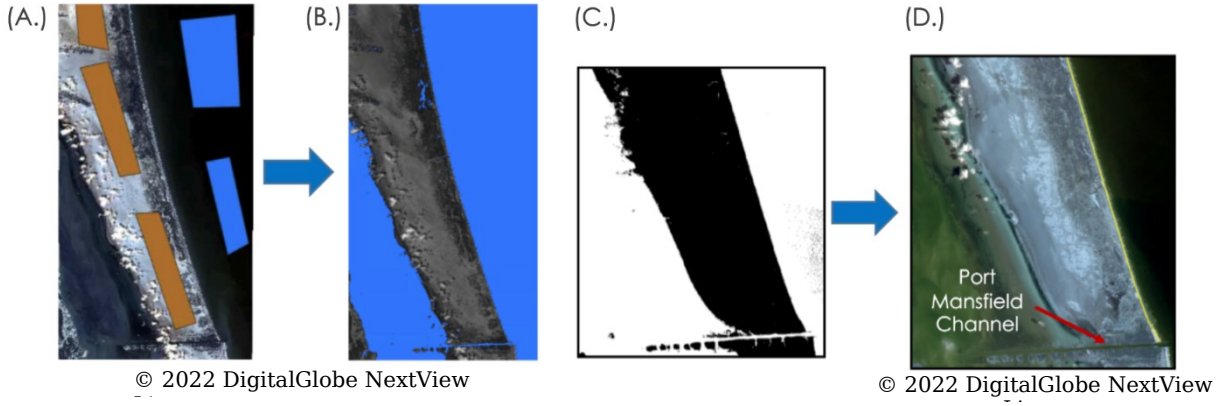


Figure 2. The diagram depicts various processing steps for classification and NDWI thresholding of the high resolution imagery: (A.) Classification training points selected for land (brown) and water (blue) to perform random forest classification, (B.) The imagery was then classified into water (blue) and land (everything else) through iso cluster classification, which was used to extract shoreline between

these two classes, (C.) A binary image that separates land and water generated from green and near-infrared (NIR) bands, which was utilized to calculate NDWI, (D.) The shoreline between land and water is extracted from the binary image and the polyline is shown in yellow.

3.3.1.1 Random Forest Classification Shoreline Extraction Methodology

Random forest classification is an algorithm that is trained with manually selected pixel value points on rasters (Figure 2A). The team utilized ENVI and the Orfeo Toolbox to select training points for land and water classes and run the classifier algorithm. After land and water were classified, the boundary between land and water was extracted and converted to a poly line, i.e., the shoreline.

3.3.1.2 Iso Cluster Classification Shoreline Extraction Methodology

The Iso Cluster Classification tool is an algorithm which separates cells of a raster into several spectrally similar classes. The tool performs unsupervised classification on all raster bands. For each date, the team utilized ArcGIS Pro and classified images into a range of 10–25 classes. The team separated these classes into land and water and utilized the reclassify tool to sort the classes into a 2 final classes (Figure 2B). After the team demarcated the land and water boundary, the classified raster was converted to a poly line to represent the shoreline. This process was repeated for each image.

3.3.1.3 NDWI Thresholding Shoreline Extraction Methodology

The team imported high-resolution imagery into ArcGIS Pro and used a shapefile of the 10-mile region north of the Port Mansfield channel to clip the raster extent. The NDWI (Equation 1) was calculated using the Band Arithmetic tool within the raster functions of ArcGIS Pro. Next, the team calculated the binary threshold of the NDWI to reduce interclass variance by using the Binary Thresholding tool within ArcGIS Pro's raster functions (Figure 2C). The resulting raster was converted to a polygon with the Raster to Polygon tool. Wave interference resulted in smaller, extraneous polygons in the coastal region. The team removed these using the Eliminate (Data Management) tool, and used the Polygon to Line tool to convert the polygon to a single poly line for each image. Before continuing to the time series analysis, the team examined and manually adjusted each poly line to reduce errors such as loops in the shoreline generated during the thresholding process for the finished product (Figure 2D).

$$NDWI = \frac{(Green - NIR)}{(Green + NIR)} \quad (1)$$

3.3.1.4 Shoreline Change Quantification Methodology

The team generated shorelines from the iso cluster classification and NDWI thresholding methodologies and did not continue with the random forest classification due to challenges in select imagery that interfered with time constraints. For the iso cluster classification and NDWI thresholding methodologies the team quantified shoreline changes in distance. First, the team created horizontal lines, with 1 km spacing, perpendicular to each shoreline.

Second, each shoreline was converted to points which intersected the perpendicular lines. Third, the team measured the distance between old and new shorelines from each intersection by using the Near (Analysis) tool in ArcGIS Pro. Shore lines that were affected by the mosaicing offset error, generated during the preprocessing steps, were shortened to exclude the impacted region.

The total area change for each time step was calculated along a ~1.4-mile strip north of the Port Mansfield Channel. The team calculated the area of the regions between old and new shorelines, for each timestep, using the Feature to Polygon tool in ArcGIS Pro. They then sorted each polygon as either a gain or loss of shoreline area. The area loss was subtracted from area gain to calculate the total area change for each year.

3.3.2 Data Analysis for Turbidity Change

The team analyzed the turbidity change with static mapping and time-series analysis. First, the team created portfolios of static maps for the years 2010 through 2020 to view turbidity trends throughout the decade in SeaDAS. Then, the team conducted method validation by comparing *in situ* turbidity measurements collected at the Bird Island Basin buoy station and the corresponding turbidity values retrieved from satellite imagery at the same location (Figure 3). After plotting retrieved turbidity values against *in situ* measurements, the team used a linear regression model to fit a line to the point cluster, and then analyzed the slope, intercept, and the deviation of fitted line from the reference line. Additionally, the team created 16 sample points along the ocean facing side of Padre Island, at which turbidity values were generated for a time series analysis. The team then used the values to generate the island's turbidity profile for comparison with shoreline change analysis.

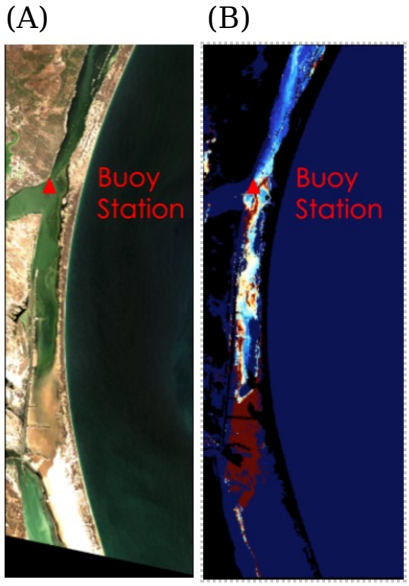


Figure 3. Depiction of the satellite imagery used and the location of where the *in situ* data is measured: (A) Original Landsat 8 Operational Land Imager (OLI) imagery of Padre Island National Seashore, (B) Final imagery after being

processed for turbidity in ACOLITE. Turbidity retrieved from satellite imagery was validated with data from the Bird Island Basin buoy station labeled by the red triangle.

4. Results & Discussion

4.1 Analysis of Results

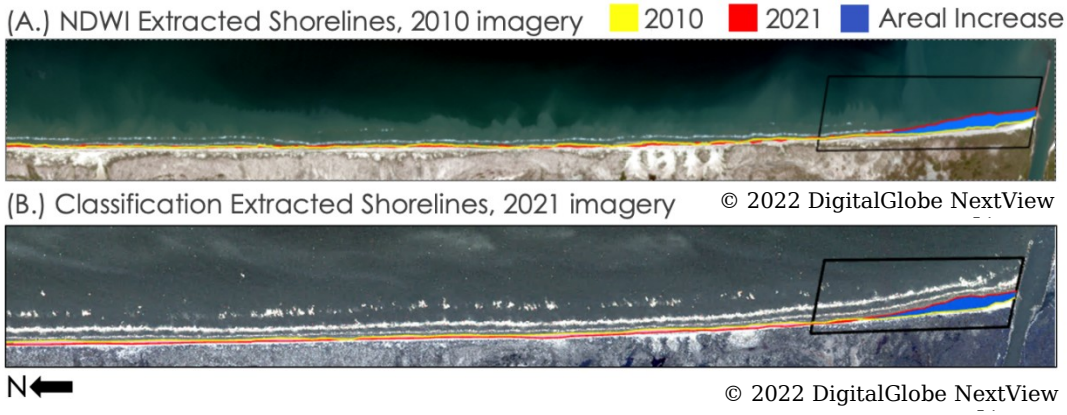
4.1.1 Shoreline Change Methodology Comparison

The team completed shoreline extraction for the years 2010 through 2021 with iso cluster classification and NDWI threshold methods. Iso cluster classification was successful in identifying land and water classes from reclassification because the study area is not geographically complex, and land and water has a major spectral difference. The con of the iso cluster algorithm was that prior to reclassification, the algorithm lacked information about what each class represents. Despite unknown classes, the team was able to interpret and reclassify the iso cluster classes into 2 classes: land and water. Random forest classification results were accurate, and representative of the given training points chosen by the team. In comparison to the unsupervised iso cluster algorithm, random forest classifier is a supervised method and sorted pixel data into known classes. However, in the team's study, the random forest algorithm had challenges in select imagery because wave pixels interfered with classification. The team was unable to complete random forest classification for each image because of time constraints of the project. The reflection of wave pixels was spectrally similar to land. The team found that the success of the NDWI method relies on the efficacy of the index selected and the selection of threshold. This method performed well in in the selected study area. Both NDWI and iso cluster classification results depicted corresponding trends in shoreline distance and area change for each year except for 2021–2022 (Figure 4 & 5). This divergence may be due to potential differences in the manual interpretations of teammates who performed manual corrections. Additionally, while utilizing the iso cluster method, the polylines were often discontinuous while the NDWI method did not have continuity issues and thus needed less manual correction. As a result, the ISO cluster may have been more accurate because it required more corrections than NDWI and because ISO lines appeared to bear more resemblance to the actual imagery.

4.1.2 Shoreline Change Results

The team separated results into two study areas. One study area, "Study Area 1", spanned 10 miles north of the Port Mansfield Channel. The second study area, "Study Area 2", spanned ~1.4 miles north of the Port Mansfield Channel and concentrates on the location where dredging efforts are focused. For both the iso cluster classification and NDWI analysis for Study Area 1, results show that the average yearly rates of shoreline distance change ranged between 4.5 to 32 meters per year (Figure 4). Notably, the highest shoreline change in Study Area 1 was between 2017–2019 while the lowest was between 2016–2017 (Figure 4C). Both methods also had similar trends in the line plot, which depict dredge events and Hurricane Hanna by gray dash lines and a green dash line respectively. The line plot shows a steady decrease in shore line changed after the 2011 dredge event. Meanwhile, shoreline change increased after the 2019 hopper dredge in response to the event. In 2020, the year Hurricane Hanna occurred, shoreline change shows

a large increase of ~25 meters, and shoreline change increased again in 2021 as multiple dredging events occur.



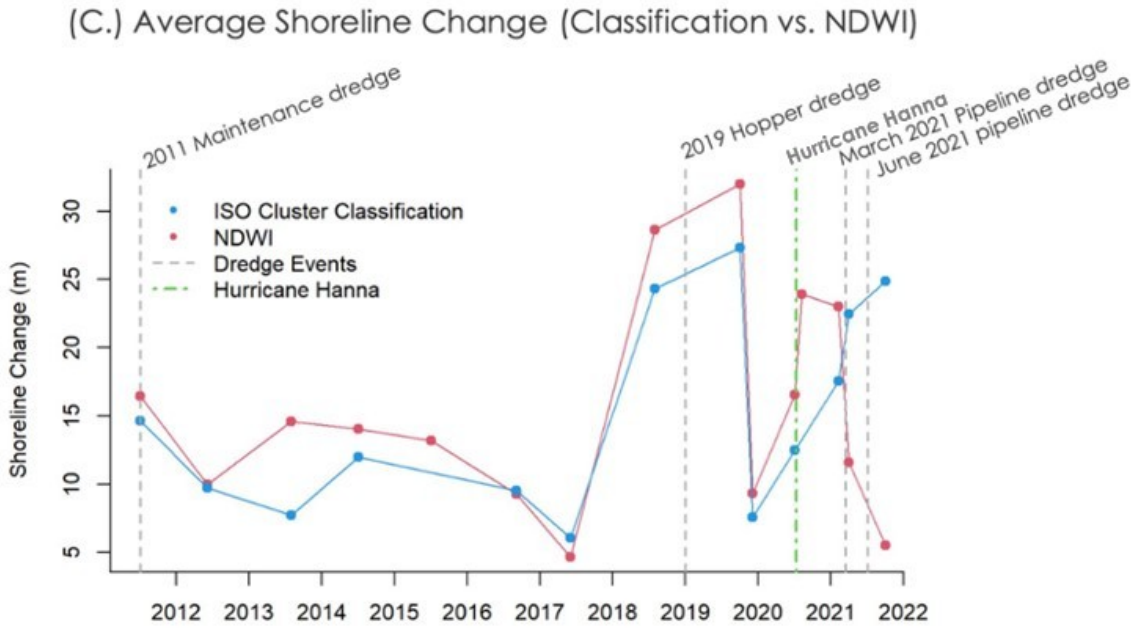


Figure 4. The results of Study Area 1: (A) 2010 NDWI extracted shorelines, (B) 2021 Classification extracted shorelines, (C) Comparison of both methods by a line plot of the average absolute shoreline change per year.

The team generated maps and graphs for Study Area 2 which depict area shoreline change in square meters. They team created time-specified maps of Study Area 2 to focus on demonstrating the effects of dredging events (Figure B1). The measurements of area changes depicted in Figure B1 are listed in Table B1. Dates that correspond to known dredging events are listed with the date range of the high-resolution imagery and the corresponding area gain and loss measurements (Table B1). The team mapped the total area change between 2010 through 2021 of Study Area 2 as displayed in Figure 5A. The team measured a total area increase of 152,000 m² between 2010 and 2021 (Figure 5A). Hurricane Hanna of 2020 was

documented by acquiring imagery for June 2020 and July 2020. Notably, during the one-month period, there was no shoreline area increase and the area decrease was 49,422 square miles. Annual areal shoreline gains and losses are shown for both iso cluster and NDWI extracted shorelines in Figure 5B and 5C.

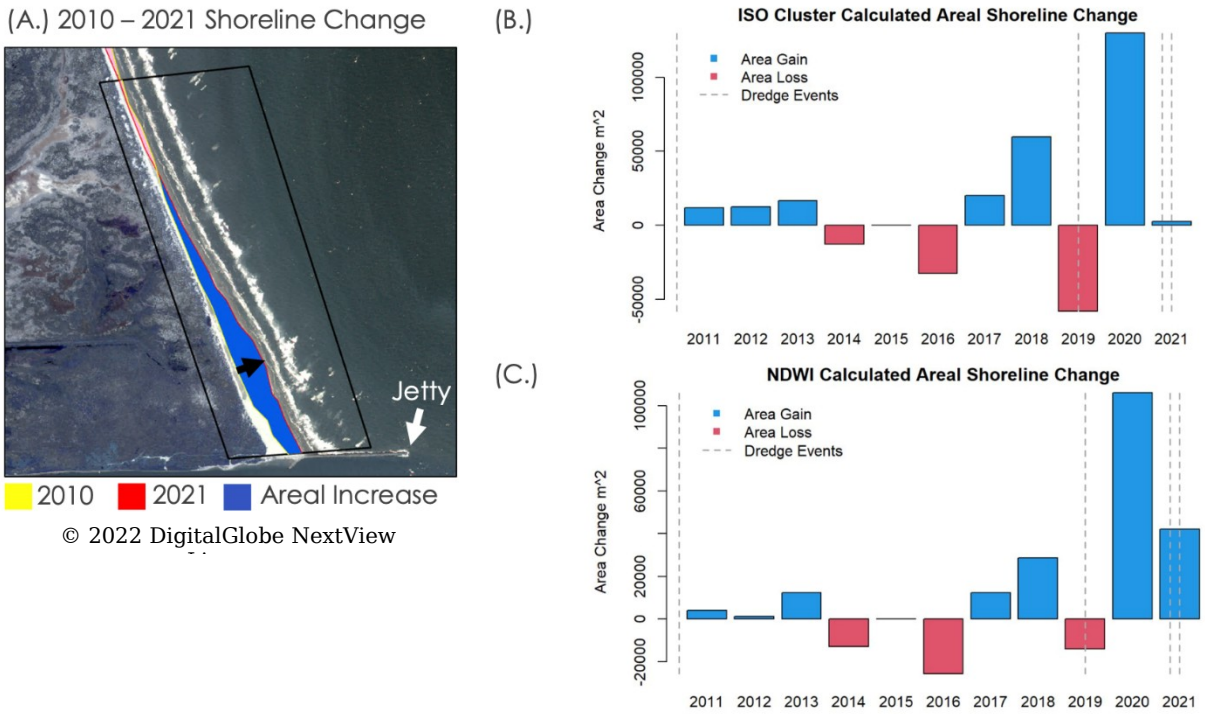


Figure 5. The area change results of Study Area 2: (A) Depicts where dredging takes place and where area shoreline change is the most variable. The arrow indicates direction of shoreline accretion. (B) A bar graph of the average area shoreline changes per year (gain or loss) for iso cluster classification shorelines. (C) A bar graph of the average area shoreline changes per year (gain or loss) for NDWI classification shorelines. 2011 is the year dredging activity in Padre Island stopped and 2019 is the year dredging activity resumed. Dredging events are indicated by dashed gray lines.

4.1.3 Turbidity Analysis Results

The validation of the Dogliotti method indicates that turbidity values were overestimated in the study area. According to Figure 6B, the linear fit is deviating from the reference line which is y equal to x. Data points below the green line indicate that the remotely sensed measurements are greater than the *in situ* measurements. One potential cause for this result is the buoy's proximity to an isle. The pixel size of Landsat imagery is 30 by 30 meters and the pixel covering the buoy could pick up signals from the bottom of the sea, which is common in nearshore areas. Based on the current validation results the team has derived, as a general turbidity retrieval method, the Dogliotti method (Dogliotti et al., 2015) isn't qualified for conducting a quantitative turbidity analysis in the study of this project but is still valid for a qualitative study. Turbidity trends were observed at 16 point locations (Figure 6A) along the nearshore environment of Padre Island

National Seashore. The historic analysis of turbidity trends shows that turbidity at Point 5, a location representative of points relatively far away from the channel, does not exhibit substantial change over the course of 15 years (Figure 6C). In contrast, for Point 15, which represents areas close to the channel and where the sand from dredging events was placed, an increase in anomalously high-turbidity measurements occur after 2015, which coincides with dredging events in 2019 and 2021(Figure 6D). The results revealed that the dredging events deployed for maintaining navigation through the channel had a notable impact on the nearshore water system through contributing a significant amount of sediments as the result of dumped sand without further nourishment being washed away by tides. It might stay neutral to the nearby water ecosystems if the solar input doesn't play a critical role in its self-sustainability. However, it's possible the increase of turbidity will reshape or even undermine the local ecosystems by limiting the incident sunlight as the main energy resource, which calls for follow-up research.

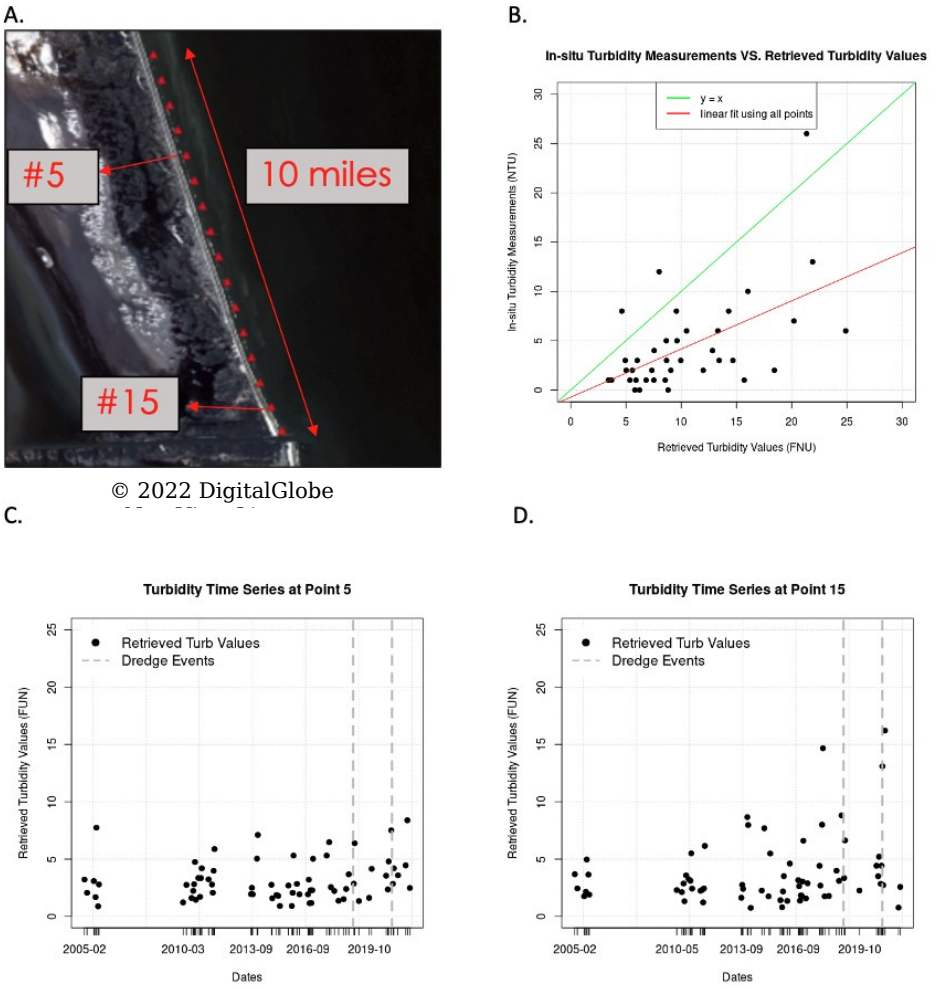


Figure 6. Turbidity analysis results: (A) A map of the 10-mile stretch of beach directly north of Port Mansfield Channel. Points in the Gulf, spaced at 1 km along the beach, are marked in red. (B) A scatter plot demonstrating the validation of retrieved turbidity measurements in comparison to *in situ* turbidity measurements from the Bird Island Basin buoy station. Points above the green line and below the red line indicate over-estimations and under-estimations of remotely sensed

turbidity, respectively, in comparison to *in situ* data. (C.) Retrieved turbidity at Point 5, a representative of areas that are relatively distant from the channel (D.) Retrieved turbidity at Point 15, a representative of areas that are close to the channel.

4.2 Errors and Uncertainties

The results of the above analyses indicate the changes to Padre Island National Seashore from beneficial use placement events utilized in the past several decades. However, these results are not without uncertainty. The analysis of turbidity in the nearshore coastal environment was validated with *in situ* data at only two inland-facing locations: Bird Island Basin and Baffin Bay. Additional *in situ* data in ocean-facing areas would have been useful for turbidity validation of the region's sediment transport trends in ocean-facing localities. The analysis was also limited by obstructed imagery, as cloud cover reduced the number of viable Landsat and Sentinel images that were usable. Additionally, sun glint interference resulted in high, invalid turbidity values. The team, therefore, omitted imagery with sun glint from the study, particularly imagery from the summer seasons, and focused on imagery from winter and fall seasons for the turbidity analysis.

For the shoreline analysis, because of tide fluctuations a lack of tidal data may have caused uncertainties in shoreline extraction and quantification. Additionally, a lack of historical dredging records impacted the team's ability to compare the amount of sediment dredged onto the beach and the amount of shoreline area change post dredging. With regards to the classification methodology, classification errors due to wave interference required an extensive removal process from the line extraction, which was completed manually. Finally, the imagery offset resulting from errors in the mosaicing process resulted in the exclusion of affected shoreline portions from the analysis.

4.3 Future Work

Future projects tracking patterns in sediment direction would be useful for understanding sediment loss and accretion before and after dredging events. This would require the use of a geostationary satellite in order to use daily or sub-daily observations of turbidity with adequate spatial and radiometric resolutions. This analysis would be useful in calculating sediment volume lost over time, which would allow for more quantitative results in relation to dredging events.

5. Conclusions

This project utilized Earth observations and remote sensing techniques to create satellite-derived products that will aid the National Park Service at Padre Island National Seashore in their upcoming beach management plans regarding beneficial use placement events along the Port Mansfield Channel. The team developed a shoreline change time series utilizing high-resolution data from both Planet and Maxar, which illustrated the changes in sediment deposition regarding dredging events that have occurred over the last decade. Based on this analysis, the team found the highest area loss in 2018, a non-dredging year. The highest area gain was in 2021, a dredging year. Additionally, Hurricane Hanna of 2020 caused the shoreline to recede by a much larger area in a 1-month period in comparison to area values the team measured for 1-year periods. In conclusion, the shoreline is affected by dredging years, and hurricanes cause the shoreline to recede in a very short time frame. The changes in shoreline and sediment deposition remain a concern for Padre Island, as both recreational and ecological use of the beach could be threatened by the erosion taking place. The analysis of the region's turbidity trends revealed that after 2015, the turbidity around the beach increases in areas close to the channel. An increase of turbidity indicates a correlation with dredging events due to the increase of sediment. The shoreline change time series and turbidity mappings will provide the partners with necessary information that will be useful in identifying the tools and locations and frequency of future dredging plans for mitigation. This will shape the local ecology and shoreline of the region.

6. Acknowledgments

The team would like to acknowledge those who supported and provided guidance for the Padre Island Water Resources project. We thank Dr. Cedric Fichot, our science advisor at Boston University, NASA DEVELOP Fellow, Tyler Pantle, and Dr. Kenton Ross at Langley Research Center. A special thanks to our Project Partners who provided us with resources and expertise throughout this project. The team would also like to thank Shelley Todd, Kelly Nesvacil, and Dr. Donna Shaver from the National Park Service, Padre Island National Seashore. Additionally, the team thanks the entirety of the DEVELOP network for support and access to resources from previous teams that have helped guide the completion of this project.

This material contains modified Copernicus Sentinel data (2015-2021), processed by ESA.

DigitalGlobe/Maxar data were provided by NASA’s Commercial Archive Data for NASA investigators (cad4nasa.gsfc.nasa.gov) under the National Geospatial-Intelligence Agency’s NextView license agreement.

PlanetScope Imagery were provided by NASA's Commercial Smallsat Data Acquisition (CSDA) Program for scientific use and Earth science applications.

Maps throughout this work were created using ArcGIS® software by Esri. ArcGIS® and ArcMap™ are the intellectual property of Esri and are used herein under license. All rights reserved.

Any opinions, findings, and conclusions or recommendations expressed in this material are those of the author(s) and do not necessarily reflect the views of the National Aeronautics and Space Administration.

This material is based upon work supported by NASA through contract NNL16AA05C.

7. Glossary

ACOLITE (Atmospheric Correction for OLI lite) – A remote sensing processing application with a specialized atmospheric correction and processing for aquatic areas with turbid coastal and inland water bodies. (The originator of ACOLITE is the Royal Belgian Institute of Natural Sciences. The software can be downloaded from the following web site: https://odnature.naturalsciences.be/remsem/software-and-data/index)
ArcGIS Pro – Geographic information system (GIS) software.
Beneficial Use Placement Events – The placement of sedimentary material (often from dredging) in areas as necessary for maintaining the geological environment.
Sentinel-2 MultiSpectral Instrument (MSI) – Satellite, operated by the European Space Agency, the sensor is the Multi-Spectral Instrument for measuring Earth's radiance.
Dredging – The removal of sediments from the bottom of water bodies to avoid sedimentation that may otherwise gradually fill channels.
Earth observations – Satellites and sensors that collect information about the Earth's physical, chemical, and biological systems over space and time.
ENVI – An image processing and analysis program.
Landsat 8 Operational Land Imager (OLI) – Satellite, operated by NASA and the USGS, the sensor is the Operational Land Imager used for measuring Earth's reflected radiance.
Landsat 5 Thematic Mapper (TM) – Satellite, operated by NASA and the USGS, the sensor is the Thematic Mapper used for measuring Earth's reflected radiance.
Maxar – Company that owns and operates WorldView-2, WorldView-3, and Geoeye-1 satellites and produced high-resolution imagery used in this research.
NAIP – United States Department of Agriculture National Agriculture Imagery Program (NAIP). Aerial imagery that was primarily utilized for georectification of the high-resolution data.
NDWI (Normalized Difference Water Index) – A remote-sensing derived index used to monitor changes in water and land by using a band ratio from green and NIR wavelengths.
Orfeo Toolbox – A remote sensing software library used in image processing.
Planet – Company that owns and operates the PlanetScope constellation of satellites and produced high-resolution imagery used in this research.
QGIS – A free and open-source cross-platform desktop geographic information system application.
SeaDAS – SeaWiFS Data Analysis Systems is an image processing and analysis program.

Turbidity – A measurement of water clarity based on suspended sediments within the water column.

8. References

Bracewell, J. 2017. Monitoring coastal topography at Gulf Coast Network parks: Protocol implementation plan – Version 1.1. Natural Resource Report NPS/GULN/NRR—2017/1522. National Park Service, Fort Collins, Colorado.

Bracewell, J. 2019. Coastal topography change at Padre Island National Seashore, Texas: 2017–2019 data summary. Natural Resource Data Series NPS/GULN/NRDS—2019/1235. National Park Service, Fort Collins, Colorado.

Domazetović, F., Šiljeg, A., Marić, I., Faričić, J., Vassilakis, E., & Panda, L. (2021) Automated Coastline Extraction Using the Very High Resolution WorldView (WV) Satellite Imagery and Developed Coastline Extraction Tool (CET). *Applied Sciences*, *11* (20), Article 9482. https://doi.org/10.3390/app11209482

Dogliotti, A. I., Ruddick, K. G., Nechad, B., Doxaran, D., & Knaeps, E. (2015). A single algorithm to retrieve turbidity from remotely-sensed data in all coastal and estuarine waters. *Remote Sensing of Environment. 156*, 157–168. https://doi.org/10.1016/j.rse.2014.09.020

European Space Agency. Copernicus Sentinel data (2015-2021). Accessed from https://earth.esa.int/web/sentinel/user-guides/sentinel-2-msi/product-types

Ghorai, D., & Mahapatra, M. (2020). Extracting Shoreline from Satellite Imagery for GIS Analysis. *Remote Sensing in Earth Systems Sciences*, *3*(1–2), 13–22. https://doi.org/10.1007/s41976-019-00030-w

Morton, R. A. (1975). Shoreline changes on Brazos Island and South Padre Island (Mansfield Channel to mouth of the Rio Grande): an analysis of historical changes of the Texas Gulf shoreline. *Virtual Landscapes of Texas*. http://dx.doi.org/10.26153/tsw/4811

Neigh, C. S. R., Masek, J. G., & Nickeson, J. (2013). High-Resolution Satellite Data Open for Government Research. *EOS Transactions*, *94*(13), 121–123. https://doi.org/10.1002/2013EO130002

Planet Team (2019, 2020, 2021). Planet Application Program Interface: In Space for Life on Earth. San Francisco, CA. https://api.planet.com

Toure, S., Diop, O., Kpalma, K., & Maiga, A. (2019). Shoreline Detection using Optical Remote Sensing: A Review. *ISPRS International Journal of Geo-Information*, *8*(2), 75. https://doi.org/10.3390/ijgi8020075

United States Department of Agriculture (USDA). Texas NAIP Imagery, 2020-04-01. Web. 2022-05-09. https://data.tnris.org/collection?c=aa5183ca-a1bd-

4b5f-9b63-4ba48d01b83d&geo=-97.6877593,26.5245017,-97.0477593,27.1645017#4.44/31.41/-100.12

U.S. Geological Survey Earth Resources Observation and Science Center. (2012). *Landsat 4-5 TM Level-1 Surface Reflectance (SR*) [Data set]. U.S. Geological Survey. https://doi.org/10.5066/P918ROHC

U.S. Geological Survey Earth Resources Observations and Science Center. (2021). *Landsat 8OLI/TIRS Level-1 Surface Reflectance (SR)* [Data set]. U.S. Geological Survey. https://doi.org/10.5066/F71835S6

Appendix A: Turbidity Processing Equation

Turbidity image processing equation from Dogliotti et al., (2015): (a) Computes the Turbidity value that associates only with one certain band (wavelength specified as sub lambda), while turbidity values derived from two bands (645 and 859) are needed to give the weights corrected turbidity value. (b) The final output of the Dogliotti method has T with no subscript as it refers to the general turbidity used in this project

Equation A1:

$$T_{\lambda} = \frac{A_T^{\lambda} \rho_w(\lambda)}{1 - \rho_w(\lambda)/C^{\lambda}} [FNU] (a)$$

$$T = (1 - w) \cdot T_{645} + w \cdot T_{859} [FNU] (b)$$

Constants

$\lambda (nm)$	A_T	C_T
645	*228.1*	*0.1641*
859	*3078.9*	*0.2112*

Symbology breakdown

Symbol	Description
T	Turbidity
ρ_w	Water Reflectance
w	Weight (Weight changes linearly from 0 at $\rho_w(645) = 0.05$ to 1 at $\rho_w(645) = 0.07$)

Appendix B

Table B1:
Known dates of dredging events from 2010–2021 are listed. The time frame of area change measurements with corresponding shoreline area gain and loss measurements are listed.

Event	Time Frame of Area Change	Shoreline Area Gain (m^2)	Shoreline Area Loss (m^2)
2011 Dredge Event	Sep. 2010 – Jul. 2011	30,870	26,846
2019 Dredge Event*	Aug. 2018 – Oct. 2019	283	41,378
2019 Dredge Event*	Oct. 2019 – Dec. 2019	27,788	731
2019 Dredge Event*	Dec. 2019 – Jun 2020	2,156	28,991
Jul. 2020 Hurricane Hanna	Jun. 2020 – Jul. 2020	0	49,422
Potential Start of 2020 Dredging Event	Jul. 2020 – Feb. 2021	139,498	0
Completion of 2021 Dredge Event in Mar.	Feb. 2021 – Apr. 2021	26,738	25,989
Jun. 2021 Dredge Event	Apr. 2021 – Oct. 2021	345	69,319

* A singular 2019 dredge event, for which multiple dates were analyzed.

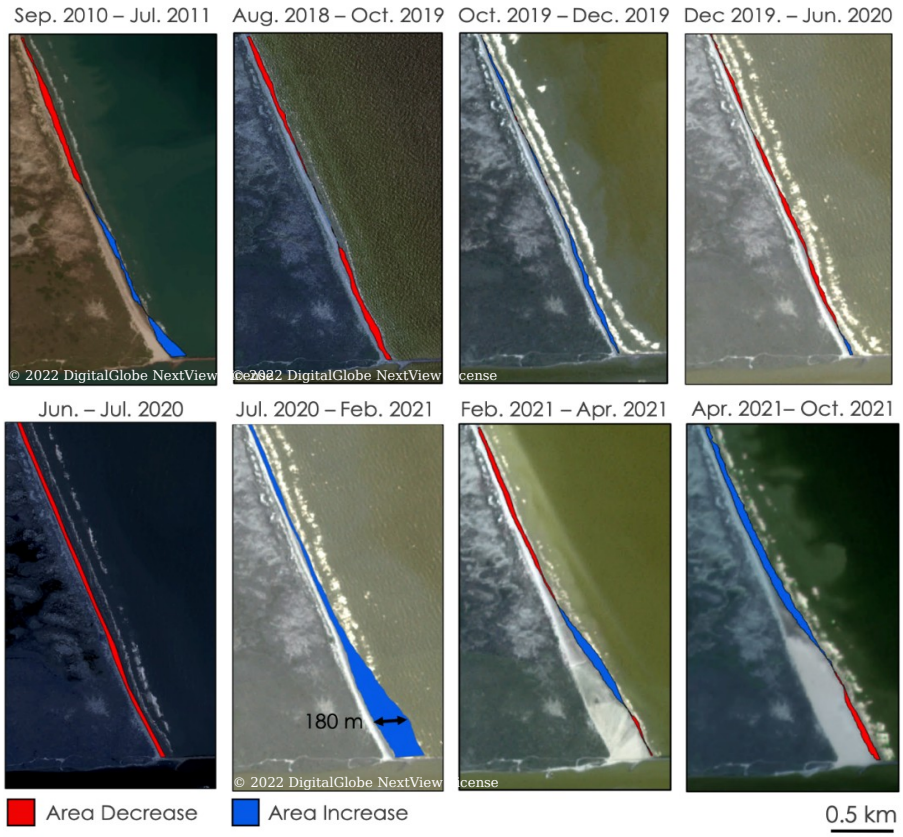


Figure B1. Maps of area increase and decrease calculated from NDWI and classification extracted shorelines. The time periods selected demonstrate shoreline change before and after dredging events and Hurricane Hanna and correspond with values in Table B1. From June to July of 2020, when Hurricane Hanna occurred, the shoreline area decreased. From July 2020 to February 2021, during a dredging event, the shoreline area increased in width by ~180m. Maxar data imagery was used for images 1, 2, and 6 under the © 2022 DigitalGlobe NextView License. PlanetScope data imagery was used for the remainder.